Kinetics and Quantitative Structure–Activity Relationships for *Pseudomonas* sp. Lipase-Catalyzed Hydrolysis of Both Monoesters and Diesters of Ethylene Glycol

Shyh-Ying Chiou[a], Yu-Ru Cheng[b], Chun-Ping Lu[c], Yan-Fu Lin[b], Long-Yau Lin[a], and Gialih Lin[b,*]

[a]Institute of Medicine and Department of Neurosurgery, Chung Shan Medical University, Taichung 402, Taiwan, and [b]Department of Chemistry and [c]Institute of Biochemistry, National Chung-Hsing University, Taichung 402, Taiwan

ABSTRACT: The goal of this work is to study kinetics and quantitative structure–activity relationships for steady states of *Pseudomonas* sp. lipase-catalyzed hydrolysis of both diesters and monoesters of ethylene glycol. Based on the steady-state kinetics of the enzyme-catalyzed hydrolysis of the diesters of ethylene glycol, the diesters and the monoesters react simultaneously as soon as monoester has started to build up in the reaction medium. In other words, the apparent K_m values of the diesters are the K_m values of the diesters (K_{mA}) plus the K_m values of the monoesters (K_{mB}), and all V_{max} values are about the same. Moreover, the pH-stat titration curve of the enzyme-catalyzed hydrolysis of the diesters of ethylene glycol is initially hyperbolic, then there is a sharp falloff in the hydrolysis rate. The abrupt stoppage of the reaction (relaxation stage) may be due to the existence of two phases in the reaction medium, that is, the product (ethylene glycol) and the substrates (the diesters of ethylene glycol) are not miscible. Furthermore, quantitative structure–activity relationships for varied acyl groups of mono- and diesters of ethylene glycol are studied. The fact that both pK_{mA} and pK_{mB} values are linearly correlated with the hydrophobicity constant (π) but not with the electronic substituent constants (σ^*) indicates that the affinity of these substrates for the enzyme depends only on the hydrophobicity of substrates.

Paper no. J11148 in *JAOCS 83,* 201–207 (March 2006).

KEY WORDS: Enzyme kinetics, esters of ethylene glycol, *Pseudomonas* sp. lipase quantitative structure–activity relationship.

The commercial potential of organic syntheses catalyzed by lipases (EC 3.1.1.3) underscores the need for a comprehensive understanding of lipase structure and function and has provided the impetus for many recent investigations (1,2). Recently, there has been increased interest in lipases owing to the use of Orlistat (Xenical®) (3). Orlistat, whose original mechanism of action consists of the selective inhibition of gastrointestinal lipases, has been commercialized for the treatment of obesity.

Lipases are lipolytic enzymes that hydrolyze ester bonds of TAG (4). However, their substrate specificity is not limited to TAG. The X-ray structures of many lipases such as *Pseudomonas cepacia* lipase and *Candida rugosa* lipase have been reported (5–10). Lipase usually contains a small α-helix or loop, referred to as the lid, that covers the active site pocket (5,7,8,11–14). This conformation is termed the closed conformation. When the lipase is absorbed to an interface, the lid is displaced so that the active site becomes accessible to substrate (15). This conformation is termed the open conformation. The structures of the free and bound lipase are believed to represent the start and end conformation in the interfacial activation process (16,17).

In general, lipases catalyze hydrolysis of TAG to 1,2-DAG, 2,3-DAG, and meso-1,3-DAG, and then also catalyze hydrolysis of these three DAG to 1-MAG, meso-2-MAG, and 3-MAG and then to glycerol. Therefore, the kinetics for lipase-catalyzed hydrolysis of TAG are very complicated owing to the many intermediates and to different stereoselectivities for some intermediates. To make the situation simple, we synthesized both diesters and monoesters of ethylene glycol (**1–6** and **7–12**, respectively) as substrates of *Pseudomonas* sp. lipase (PSL) and characterized their kinetics.

The first reaction in the PSL-catalyzed hydrolysis of diesters **1–6** is formation of monoesters **7–12** (Fig. 1). Then the enzyme catalyzes a subsequent reaction *in situ* to hydrolyze monoesters **7–12** to ethylene glycerol (EG). Thus, the subsequent hydrolysis of diesters **1–6** *in situ* will be the same as the hydrolysis of monoesters **7–12** to EG.

Figure 1 represents a Ping Pong Bi Bi mechanism. In the absence of products P and Q, the forward velocity is given by Equation 1 (18):

$$v = V_{max}\,[A]\,[B]/(K_{mB}\,[A] + K_{mA}\,[B] + [A]\,[B]) \qquad [1]$$

For the hydrolysis of diesters **1–6**, the diesters (A) and the monoesters (B) may react simultaneously as soon as some monoester has started to build up in the reaction medium. Then [A] = [B] and Equation 1 becomes Equation 2.

$$v = V_{max}\,[A]/((K_{mA} + K_{mB}) + [A]) \qquad [2]$$

In other words, the apparent K_m values of the diesters are the K_m values of the diesters (K_{mA}) plus the K_m values of the monoesters (K_{mB}), and the V_{max} values are constant.

Furthermore, quantitative structure–activity relationships (19) for varied acyl substituents of diesters **1–6** and monoesters

*To whom correspondence should be addressed.
E-mail: gilin@dragon.nchu.edu.tw

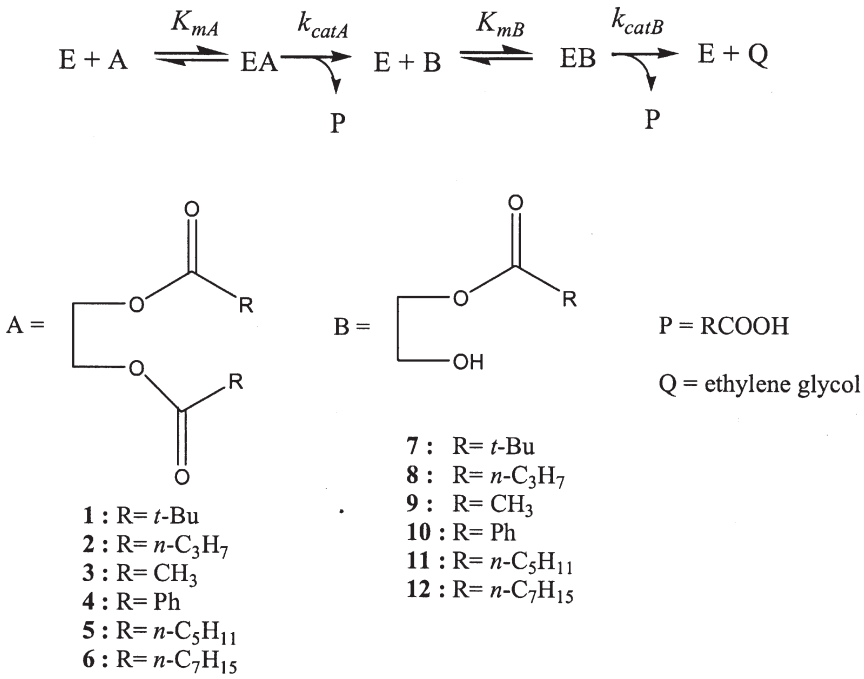

FIG. 1. Kinetic scheme for the *Pseudomas* sp. lipase (PSL)-catalyzed hydrolysis of diesters **1–6** to monoesters **7–12,** then the PSL-catalyzed hydrolysis of monesters **7–12** to ethylene glycol. A, the diesters of ethylene glycol (**1–6**); B, the monoesters of ethylene glycol (**7–12**); E, enzyme; EA, enzyme-**1–6** tetrahedral complex; EB, enzyme-**7–12** tetrahedral complex; K_{mA}, Michaelis constant of **1–6**; K_{mB}, Michaelis constant of **7–12**; k_{catA}, turnover number of **1–6**; k_{catB}, turnover number of **7–12**; P, the first product (FA); Q, the second product (ethylene glycol).

7–12 may provide us much information to characterize these reaction mechanisms.

EXPERIMENTAL PROCEDURES

Materials. PSL was obtained from Sigma (St. Louis, MO); other chemicals were obtained from Aldrich (Milwaukee, WI). Silica gel used in LC (LiChroprep Silica 60, 200–400 mesh) and TLC plates (Kieselgel 60 F_{254}) were obtained from Merck (Darmstadt, Germany). A hexane/ethyl acetate solvent gradient was used in LC. Other chemicals were of the highest quality available commercially.

Synthesis of substrates. The diesters of ethylene glycol (**1–6**) and the corresponding monoesters of ethylene glycol (**7–12**) were synthesized in one-step reactions. The reaction of ethylene glycol with 2 equiv of acyl chloride in the presence of 2 equiv of sodium hydride (NaH) in THF at 25°C for 24 h yields diesters **1–6** and the corresponding monoesters **7–12**. Diesters **1–6** (45–50% yield) and the corresponding monoesters **7–12** (45–50% yield) were then separated and purified by LC. A typical reaction for synthesis of 1,2-dibenzoxy-ethane (**4**) and 2-benzoxy-ethanol (**10**) may be described as follows. Reaction of ethylene glycol with 2 equiv of benzoyl chloride in the presence of 2 equiv of NaH in THF at 25°C for 24 h yields **4** and **10**. Compounds **4** (47% yield) and **10** (45% yield) were separated and purified by LC.

Compounds **1–12** were characterized by ^{1}H and ^{13}C NMR spectra, mass spectra, and elemental analysis.

Instrumental methods. All kinetic data were obtained from a pH-stat titration apparatus that was composed of a pH-stat controller (PHM 290; Radiometer) and an autoburette (AUB 901; Radiometer) with a circulating water bath jacket. ^{1}H and ^{13}C NMR spectra were recorded at 400.45 and 100.70 MHz, respectively (Varian Gemini 400 spectrometer). The ^{1}H and ^{13}C NMR chemical shifts were referred to internal tetramethylsilane. Mass spectra were recorded at 70 eV on a Joel JMS-SX/SX-102A mass spectrometer. Elemental analysis was performed on a Heraeus instrument.

Data reduction. Origin (version 6.0; OriginLab, Northampton, MA) was used for both linear and nonlinear least-squares curve fittings.

Enzyme kinetics. All kinetic data were obtained by using a pH-stat titration apparatus that was interfaced to a personal computer. Temperature was maintained at 25.0°C by a circulating water bath. All reactions were performed in a NaCl (0.1 M) solution with varying concentration of the substrates **1–12**. Reactions were initiated by injecting PSL into a stock solution of substrate. The reactions were titrated from the autoburette, which contained 0.001 M NaOH, and the pH-stat controller was set at pH = 8.0. The steady-state initial velocities (v) for PSL-catalyzed hydrolysis of **1–12** were determined as the initial slopes from the initial hyperbolic curves of the time courses

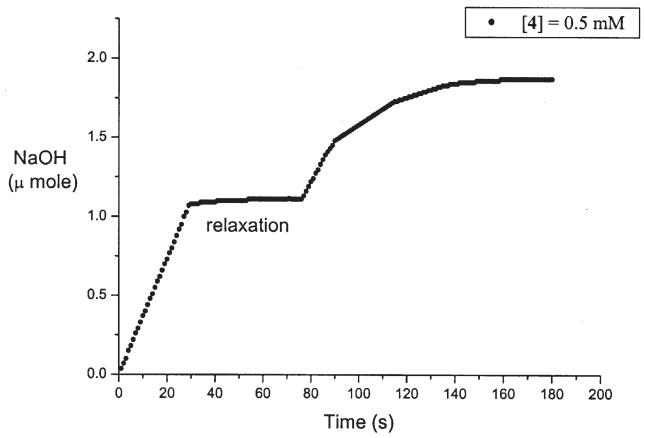

FIG. 2. Time course of pH-stat titration of PSL-catalyzed hydrolysis of **4**. The overall time course consisted of (i) the initial hyperbolic curve and (ii) the relaxation stage. The reactions were titrated with 0.001 M NaOH, and the pH-stat controller was set at pH = 8.0. [**4**] = 0.5 mM. v = 1.2 μmol/s. The lifetime of the relaxation stage is 50 s. For abbreviation see Figure 1.

(Fig. 2). The K_{mB} and V_{maxB} values (Table 1) for PSL-catalyzed hydrolysis of monoesters **7–12** were obtained from the nonlinear least-squares curve fitting of v vs. the concentration of monoesters **7–12** ([B]) plot against the Michaelis–Menten equation. The $K_{mA} + K_{mB}$ and V_{maxA} values (Table 2) for PSL-catalyzed hydrolysis of diesters **1–6** were obtained from the nonlinear least-squares curve fitting of v vs. the concentration of diesters **1–6** ([A]) plot against Equation 2 (18). Duplicate sets of data were collected for each substrate concentration.

Relaxation rate (k_{relax}). The relaxation rate ($k_{relax.}$) for the PSL-catalyzed hydrolysis of diesters **7–12** was determined as $1/t_{relax}$, where t_{relax} is the lifetime of the relaxation stage (Fig. 2).

RESULTS AND DISCUSSION

The diesters of ethylene glycol (**1–6**) and the monoesters of ethylene glycol (**7–12**) were synthesized as simple analogs of TAG, DAG, and MAG.

The v values for the PSL-catalyzed hydrolysis of diesters **1–6** and monoesters **7–12** were obtained from the initial slopes of the pH-stat titration time courses. The K_{mB} and V_{maxB} values for the PSL-catalyzed hydrolysis of monoesters **7–12** were obtained from the nonlinear least-squares curve fittings of v vs. substrate concentration plots against the Michaelis–Menten equation (Table 1). The $K_{mA} + K_{mB}$ and V_{maxA} values (Table 2) for the PSL-catalyzed hydrolysis of diesters **1–6** were obtained from the nonlinear least-squares curve fittings of v vs. substrate concentration plots against Equation 2 (18). Therefore, K_{mA} was calculated by subtracting K_{mB} from $K_{mA} + K_{mB}$.

The pK_{mA}, pK_{mB}, log (V_{maxA}/K_{mA}), and log (V_{maxB}/K_{mB}) values were linearly correlated with the hydrophobicity constant (π) (19) (Fig. 3, Table 3); however, these values were not linearly correlated with the electronic substituent constants σ* (Fig. 4).

TABLE 1
Kinetic Data for Pre-Steady and Steady States of PSL-Catalyzed Hydrolysis of the Monoesters of Ethylene Glycol[a] (7–12)

Substrate	R	K_{mB} (mM)	V_{maxB} (nmol/s)	V_{maxB}/K_{mB} (10^{-3} mol s^{-1} M^{-1})
7	*t*-Bu	0.15 ± 0.01	48.1 ± 0.2	0.32 ± 0.02
8	*n*-C_3H_7	1.5 ± 0.2	49 ± 1	0.033 ± 0.004
9	CH_3	10 ± 1	47 ± 1	0.0047 ± 0.0005
10	Ph	0.26 ± 0.07	48.3 ± 0.7	0.19 ± 0.05
11	*n*-C_5H_{11}	0.15 ± 0.1	48.2 ± 0.8	0.32 ± 0.02
12	*n*-C_7H_{15}	0.10 ± 0.01	47.5 ± 0.1	0.48 ± 0.05

[a]PSL, *Pseudomonas* sp. lipase.

TABLE 2
Substituent Constants and Steady-State Kinetic Data of PSL-Catalyzed Hydrolysis of the Diesters of Ethylene Glycol (1–6)

Substrate	R	σ*[a]	π[a]	K_{mA} (mM)	V_{maxA} (nmol/s)	V_{maxA}/K_{mA} (10^{-3} mol s^{-1} M^{-1})
1	*t*-Bu	−0.3	1.98	1.7 ± 0.3	40.6 ± 0.3	0.024 ± 0.004
2	*n*-C_3H_7	−0.1	1.5	0.30 ± 0.05	38.9 ± 0.6	0.13 ± 0.02
3	CH_3	0	0.5	3.0 ± 0.3	45 ± 3	0.015 ± 0.002
4	Ph	0.6	2.13	0.10 ± 0.03	49 ± 1	0.49 ± 0.01
5	*n*-C_5H_{11}	−0.13	2.5	0.19 ± 0.04	45 ± 1	0.24 ± 0.05
6	*n*-C_7H_{15}	−0.13	3.5	0.13 ± 0.04	47 ± 1	0.4 ± 0.1

[a]Taken from References 19–22. σ*, electronic substituent constants; π, hydrophobicity constants; for other abbreviation see Table 1.

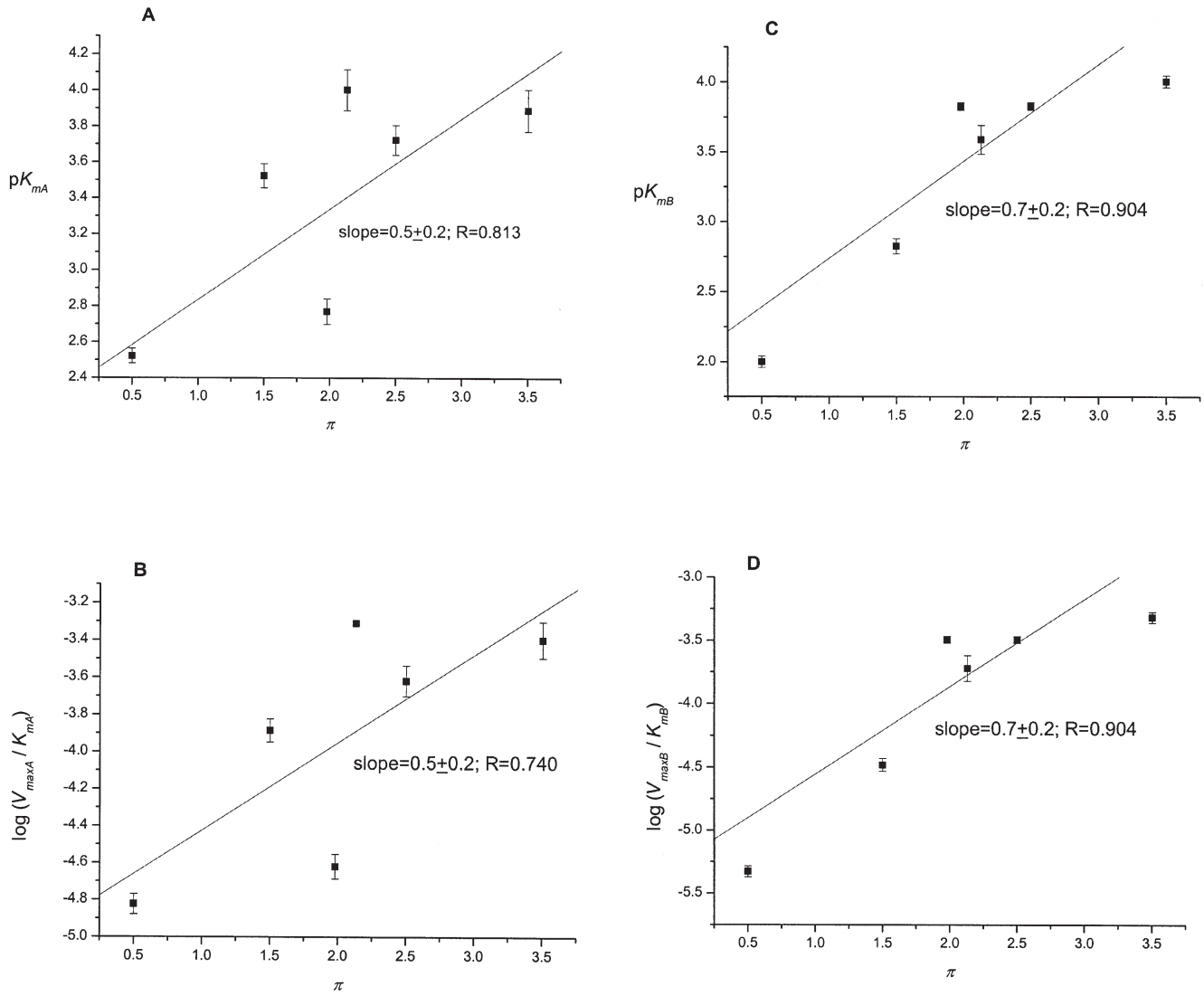

FIG. 3. Plots of (A) pK_{mA}, (B) log (V_{maxA}/K_{mA}), (C) pK_{mB}, and (D) log (V_{maxB}/K_{mB}) values for PSL-catalyzed hydrolysis of diesters **1–6** and monoesters **7–12** against π, the hydrophobicity constant. Correlation results are summarized in Table 3. For abbreviation see Figure 1.

The pH-stat titration curve of the enzyme-catalyzed hydrolysis of diesters **1–6** consisted of a hyperbolic curve, then a sharp falloff in the hydrolysis rate (Fig. 2). The abrupt stoppage of the reaction was a relaxation stage with the rate constant of k_{relax}. The log k_{relax} values were linearly correlated with π (Fig. 5).

Based on the steady-state kinetics of the enzyme-catalyzed hydrolysis of diesters **1–6** (Table 2), the diesters and the monoesters react simultaneously as soon as some monoester has been built up in the reaction medium. In other words, the apparent K_m values of the diesters are the K_m values of the diesters

TABLE 3
Results of the Linear Correlations of pK_{mA}, log (V_{maxA}/K_{mA}), pK_{mB}, log (V_{maxB}/K_{mB}), and log k_{relax} with π

	pK_{mA}	log (V_{maxA}/K_{mA})	pK_{mB}	log (V_{maxB}/K_{mB})	log k_{relax}
h^a	2.3 ± 0.3	−4.9 ± 0.5	1.9 ± 0.4	−5.4 ± 0.4	−1.43 ± 0.02
y^b	0.5 ± 0.2	0.5 ± 0.2	0.7 ± 0.2	0.7 ± 0.2	−0.124 ± 0.008
R^c	0.813	0.740	0.904	0.904	0.992
SEM	0.187	0.196	0.152	0.152	0.007

[a]Intercept for the pK_{mA}, log (V_{maxA}/K_{mA}), pK_{mB}, log (V_{maxB}/K_{mB}), or log k_{relax} values vs. π plot (Figs. 2, 4).
[b]Slopes for the pK_{mA}, log (V_{maxA}/K_{mA}), pK_{mB}, log (V_{maxB}/K_{mB}), or log k_{relax} values vs. π plot (Figs. 2, 4).
[c]Correlation coefficient. For abbreviations see Table 2.

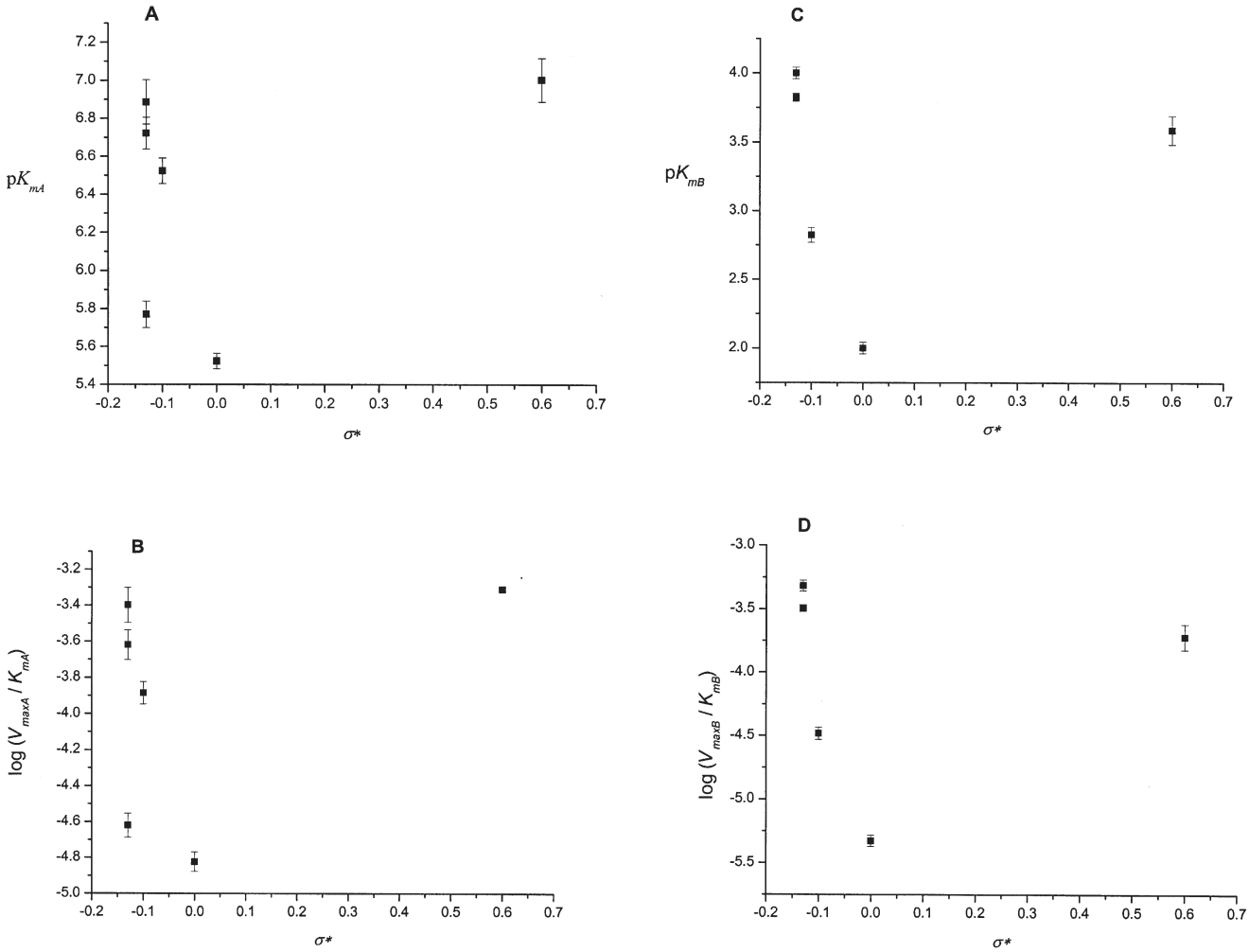

FIG. 4. Plots of (A) pK_{mA}, (B) log (V_{maxA}/K_{mA}), (C) pK_{mB}, and (D) log (V_{maxB}/K_{mB}) values for PSL-catalyzed hydrolysis of diesters **1–6** and monoesters **7–12** against electronic substituent constants σ*. For abbreviation see Figure 1.

(K_{mA}) plus the K_m values of the monoesters (K_{mB}). The fact that the V_{maxA} and V_{maxB} values (Tables 1 and 2) are about the same indicates that the PSL-catalyzed hydrolysis of diesters **1–6** proceeds with the Ping Pong Bi Bi mechanism (Fig. 1) (18). For the PSL-catalyzed hydrolysis of diesters **1–6**, the product of the first reaction, monoesters **7–12**, are instantly excluded from the active site of the enzyme then quickly diffuse into the active site (Fig. 6).

The fact that the pK_{mA}, pK_{mB}, log (V_{maxA}/K_{mA}), and log (V_{maxB}/K_{mB}) values were linearly correlated with π (Fig. 3, Table 3) but not with σ* (Fig. 4) indicates that the PSL-catalyzed hydrolysis of diesters **1–6** and monoesters **7–12** only depends on the hydrophobicity of the substrates. The ψ value (i.e., the slope of the log *k* vs. p plot) of 0.5 or 0.7 for the pK_{mA}- or pK_{mB}-π-correlation (Table 3) implies that the enzyme–substrate tetrahedral intermediates are more stabilized by a hydrophobic acyl moiety than a hydrophilic acyl moiety (20–23). This is probably due to strong van der Waals' or hydrophobic interactions between the acyl moiety of the substrate and the acyl chain binding site (6) of the enzyme (Fig. 6). The fact that the ψ values for the log (V_{maxA}/K_{mA})–π-correlation and the pK_{mA}–π-correlation (Table 3) are about the same suggests that the ψ value

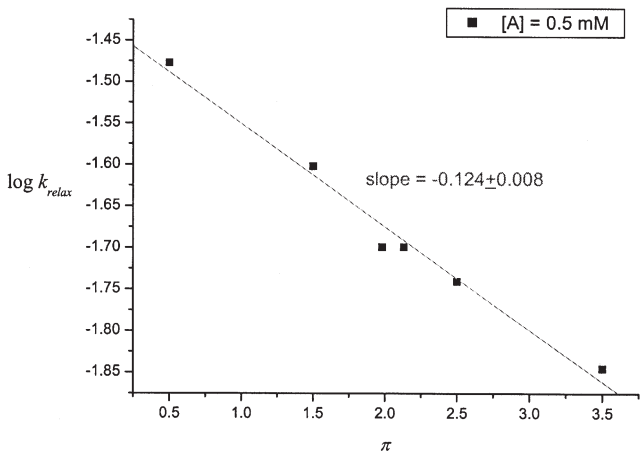

FIG. 5. Plot of the log $k_{relax.}$ values for PSL-catalyzed hydrolysis of diesters **1–6** against π. For abbreviation see Figure 1.

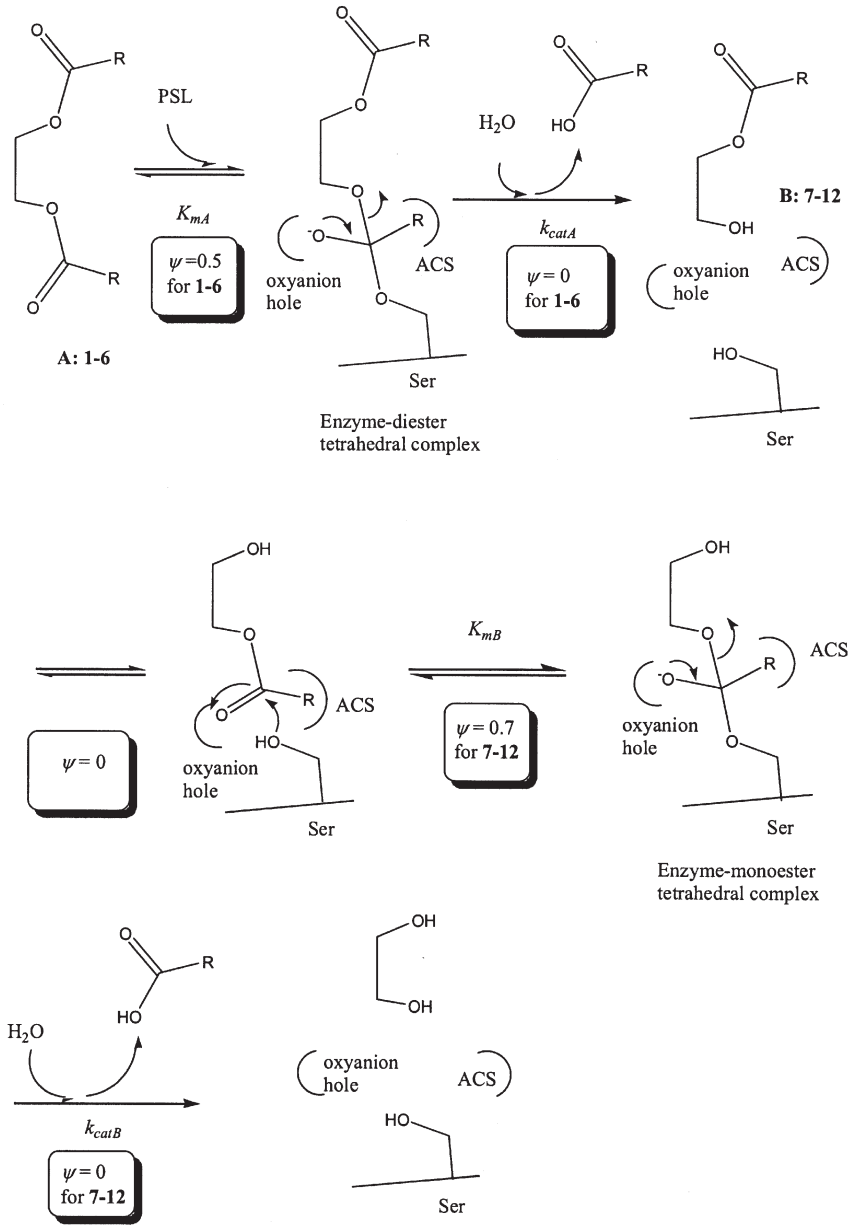

FIG. 6. Proposed mechanism for PSL-catalyzed hydrolysis of diesters **1–6** to ethylene glycerol. The first step (K_{mA}) is formation of the enzyme–diester tetrahedral complex. The second step (k_{catA}) involves formation of monoester **7–10** as the first product of the reaction and then formation of the second product, FA. The third step is diffusion of the monoesters **7–10** into the active site of the enzyme. The fourth step (K_{mB}) involves the formation of the enzyme–monoester tetrahedral complex. The fifth step (k_{caB}) involves the formation of ethylene glycol. ψ, slope for log *k* vs. π plot; ACS, acyl chain binding site; for other abbreviation see Figure 1.

for the log k_{catA}–π-correlation is about zero (Fig. 6). Since the k_{catA} step consists of two steps, formation of the acyl enzyme from the tetrahedral intermediate and hydrolysis of the acyl enzyme to products, the ψ values for above two steps seem to cancel each other. For similar reasons, the ψ value for the log k_{catB}–π-correlation is about zero (Fig. 6).

Moreover, the pH-stat titration curve of PSL-catalyzed hydrolysis of diesters **1–6** consists of a hyperbolic curve, then a sharp falloff in the hydrolysis rate (Fig. 2). The abrupt stoppage of the reaction (relaxation stage) may be due to a change in the physical state of the reaction medium. In other words, the relaxation stage may be due to the existence of two phases in the reaction medium, that is, the product (EG) and the substrates (diesters **1–6**) are not miscible (Fig. 7). Furthermore, the log k_{relax} values are correlated with π (Fig. 5, Table 3). The ψ value of –0.124 for the above correlation indicates that more hydrophobic diesters such as **5** and **6** have longer relaxation times than less hydrophobic diesters such as **2** and **3**.

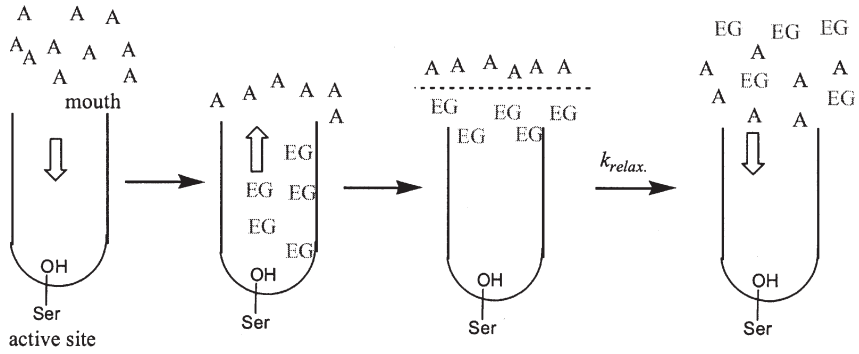

FIG. 7. Proposed mechanism for the relaxation process in the PSL-catalyzed hydrolysis of diesters **1–6**. The first step is hydrolysis of diesters **1–6** (substrate A). The second step involves diffusion of ethylene glycerol (EG) out of the active site to form a biphasic medium. In this medium, substrate A cannot enter the active site of the enzyme owing to the hindrance at the mouth of the enzyme by the aggregation of EG. The third step ($k_{relax.}$) is the relaxation process, which breaks down the biphasic medium. Therefore, substrate A enters the active site of the enzyme following this relaxation or emulsification.

REFERENCES

1. Boland, W., C. Frößl, and N. Lorenz, Esterolytic and Lipolytic Enzymes in Organic Synthesis, *Synthesis 12*:1049–1072 (1991).
2. Theil, F., Lipase-Supported Synthesis of Biologically Active Compounds, *Chem. Rev. 95*:2203–2227 (1995).
3. Drent, M.L., and E.A. Vanderveen, First Clinical Studies with Orlistat: A Short Review, *Obes. Res. 3*:S623–S625 (1995).
4. Svendsen, A., Sequence Comparison with the Lipase Family, in *Lipases. Their Structure Biochemistry and Application*, edited by P. Woolley and S.B. Petersen, Cambridge University Press, Cambridge, 1994, pp. 1–21.
5. van Tilbeurgh, H., M.-P. Egloff, C. Martinez, N. Rugani, R. Verger, and C. Cambillau, Interfacial Activation of the Lipase-Procolipase Complex by Mixed Micelles Revealed by X-ray Crystallography, *Nature 362*:814–820 (1993).
6. Lang, D.A., M.L.M. Mannesse, G.H. DeHaas, H.M. Verheij, and B.W. Dijkstra, Structural Basis of the Chiral Selectivity of *Pseudomonas cepacia* Lipase, *Eur. J. Biochem. 254*:333–340 (1998).
7. Schrag, J.D., Y. Li, M. Cygler, D. Lang, T. Burgdorf, H.-J. Hecht, R. Schmid, D. Schomburg, T.J. Rydel, J.D. Oliver, L.C. Strickland, C.M. Dunaway, S.B. Larson, J. Day, and A. McPherson, The Open Conformation of *Pseudomonas* Lipase, *Structure 5*:187–202 (1997).
8. Kim, K.K., H.K. Song, D.H. Shin, K.Y. Hwang, and S.W. Suh, The Crystal Structure of a Triacylglycerol Lipase from *Pseudomonas cepacia* Reveals a Highly Open Conformation in the Absence of a Bound Inhibitor, *Structure 5*:173–185 (1997).
9. Grochulski, P., F. Bouthillier, R.J. Kazlauskas, A.N. Serreqi, J.D. Schrag, E. Ziomek, and M. Cygler, Analogs of Reaction Intermediates Identify a Unique Substrate Binding Site in *Candida rugosa* Lipase, *Biochemistry 33*:3494–3500 (1994).
10. Luic, M., S. Tomic, I. Lescic, E. Liubovic, D. Sepac, V. Sunjic, L. Vitale, W. Saenger, and B. Kojic-Prodic, Complex of *Burkholderia cepacia* Lipase with Transition State Analogue of 1-Phenoxy-2-acetoxybutane. Biocatalytic, Structural and Modelling Study, *Eur. J. Biochem. 268*:3964–3973 (2001).
11. Brady, L., A.M. Brzozowski, Z.S. Derewenda, E. Dodson, G. Dodson, S. Tolley, J.P. Turkenburg, L. Christiansen, B. Huge-Jensen, L. Norskov, L. Thim, and U. Menge, A Serine Protease Triad Forms the Catalytic Center of a Triacylglycerol Lipase, *Nature 343*:767–770 (1990).
12. Pleiss, J., M. Fischer, and R.D. Schmid, Anatomy of Lipase Binding Sites: The Scissile Fatty Acid Binding Site, *Chem. Phys. Lipids 93*:67–80 (1998).
13. Cavalier, J.-F., G. Buono, and R. Verger, Covalent Inhibition of Digestive Lipases by Chiral Phosphates, *Acc. Chem. Res. 33*:579–589 (2000).
14. Svendsen, A., Lipase Protein Engineering, *Biochim. Biophys. Acta 1543*:223–238 (2000).
15. Brzozowski, A.M., U. Derewenda, Z.S. Derewenda, G.G. Dodson, D.M. Lawson, J.P. Turkenburg, F. Bjorkling, B. Huge-Jensen, S.A. Patkar, and L. Thim, A Model for Interfacial Activation in Lipase From Structure of a Fungal Lipase–Inhibitor Complex, *Nature 351*:491–494 (1991).
16. Derewenda, Z.S., A Twist in the Tale of Lipolytic Enzymes, *Nat. Struct. Biol. 2*:347–349 (1995).
17. Berg, O.G., M.H. Gelb, M.-D. Tsai, and M.K. Jain, Interfacial Enzymology: The Secreted Phospholipase A_2-Paradigm, *Chem. Rev. 101*:2613–2653 (2001).
18. Segel, I.H., *Enzyme Kinetics*, John Wiley & Sons, New York, 1975.
19. Isaacs, N., *Physical Organic Chemistry*, 2nd edn., Longman, Harlow, Essex, United Kingdom, 1995.
20. Lin, G., C.-T. Shieh, H.-C. Ho, J.-Y. Chouhwang, W.-Y. Lin, and C.-P. Lu, Structure–Reactivity Relationships for the Inhibition Mechanism at the Second Alkyl Chain Binding Site of Cholesterol Esterase and Lipase, *Biochemistry 38*:9971–9981 (1999).
21. Lin, G., G.-H. Chen, Y.-F. Lin, L.-H. Su, and P.-S. Liao, Highly Potent and Selective 4,4′-Biphenyl-4-acylate-4′-*N*-*n*-butylcarbamate Inhibitors as *Pseudomonas species* Lipase. *Eur. J. Lipid Sci. Technol. 107*:65–73 (2005).
22. Lin, G., and G.-Y. Yu, QSAR for Phospholipase A_2 Inhibitions by 1-Acyloxy-3-*N*-*n*-octylcarbamyl-benzenes, *Bioorg. Med. Chem. Lett. 15*:2405–2408 (2005).

[Received June 3, 2005; accepted December 2, 2005]